Hindawi
Journal of Nanomaterials
Volume 2020, Article ID 2901516, 10 pages
https://doi.org/10.1155/2020/2901516

Research Article

N-TiO_{2-x} Nanocatalysts: PLAL Synthesis and Photocatalytic Activity

Enza Fazio,[1] **Angela Maria Mezzasalma**,[1] **Luisa D'Urso**,[2] **Salvatore Spadaro**,[1] **Francesco Barreca**,[1] **Giovanni Gallo**,[1] **Fortunato Neri**,[1] **and Giuseppe Compagnini**[2]

[1]*Dipartimento di Scienze Matematiche e Informatiche, Scienze Fisiche e Scienze della Terra (MIFT), Università di Messina, Viale Ferdinando Stagno d'Alcontres 31 98166 Messina, Italy*
[2]*Dipartimento di Scienze Chimiche, Università di Catania, Viale Andrea Doria 6, 95125 Catania, Italy*

Correspondence should be addressed to Giuseppe Compagnini; gcompagnini@unict.it

Received 27 February 2020; Revised 5 May 2020; Accepted 7 May 2020; Published 11 June 2020

Academic Editor: Kishore Sridharan

N-TiO_{2-x} nanocatalysts are developed by the pulsed laser ablation in liquid (PLAL) technique, a simple and surfactant-free preparation method. The PLAL approach allows synthesizing chemical-morphological fine-tuning water TiO_2-based nanomaterials, starting from targets of different nature (powders and commercial high purity targets). The catalytic activity was investigated using methylene blue (cationic dye) and methyl orange (azo dye). A different photocatalytic response was found for the various kinds of N-TiO_{2-x}. In the first 20 min, under UV and visible light, about 50% and 10% of the methyl orange were removed using the N-TiO_{2-x} and TiO_2 colloids, respectively. In addition, we observe that the response towards the methylene blue is comparable in all the synthesized samples under UV irradiation while differing by about 30% under a visible lamp. The enhanced photocatalytic response of the N-TiO_{2-x} nanocatalysts with respect to the TiO_2 one is dependent on the content of the nitrogen dopant, surface area, and nitrogen-oxygen bonding configurations.

1. Introduction

TiO_2 is extensively studied in view of photocatalytic applications thanks to its low cost, high photogenerated hole oxidizing power, and long lifetime of electron/hole pairs when irradiated with light. Such photoinduced electron-hole pairs have been utilized to generate electricity in solar cells, to split water into hydrogen and oxygen, and to oxidize and degrade inorganic/organic/biological compounds in environments as well as to create superhydrophilicity [1].

The first reliable paper on photocatalytic activity of TiO_2 was published in 1938. It has been shown that UV absorption produced active oxygen species on TiO_2 surfaces, causing photobleaching of dyes [2]. Subsequent works to this have shown the oxidation of organic solvents and the formation of H_2O_2 under an UV irradiation of a mercury lamp under ambient conditions while the water photolysis was demonstrated for the first time in 1969 on TiO_2 semiconductors [3]. Fundamental processes of TiO_2 photoelectrochemistry have been studied intensively, mainly analyzing the behavior of TiO_2 nanomaterials, interesting for their high surface-volume ratio. TiO_2 nanostructures provide increased surface area at which photoinduced reactions may occur, enhancing the light absorption rate, increasing the surface photoinduced carrier density, enhancing the photoreduction rate, and resulting in higher surface photoactivity. At the same time, the high surface-volume ratio of the nanoparticles enhances the surface absorption of OH− and H_2O, increasing the photocatalytic reaction rate [4, 5]. Based on the basic research results, industrial applications of photocatalytic TiO_2 have been achieved since the end of the 1990s and will develop further in the 21st century. Among them are photocatalytic water splitting [6], purification of pollutants [7], photocatalytic self-cleaning [8], photocatalytic antibacteria,

and photoinduced super hydrophilicity [9], as well as photovoltaics and photosynthesis [10] (see Figure 1).

However, the large bandgap of TiO_2 (3.2 eV for anatase and 3 eV for rutile) limits its light absorption only to the UV region [11]. Thus, pure TiO_2 works as a photocatalytic material under UV light (4-5% of solar light), but it has very low photocatalytic activity in visible light (45% of solar spectrum). Some efforts have been made to overcome this limitation. Some aspects have been identified as essential to resolve the issue such as to tailor TiO_2 bulk/surface electronic structures and the interfaces in order to tune surface band-bending, surface state distribution, and charge separation, which could significantly influence TiO_2 photocatalysis response in the visible spectral range. The main requirements are (1) a high surface/volume ratio and a controlled anatase-rutile ratio to provide a large number of active sites for the degradation reaction and (2) shifting the absorption limit of the material in the visible range, searching for an increase in reaction rate of photocatalysis and hydrogen production.

Doping appears as a good alternative for changing the activity of TiO_2 catalysts through the optoelectrical modification of this material by the introduction of dopants with different energy levels between the conduction and valence bands. The applied dopants can be (1) noble metals (such as Ag, Au, Pd, and Pt), which absorb the visible light due to the surface plasmon resonance, but the high cost associated with these materials should be considered a disadvantage [12]; (2) transition metals cheaper than noble metals, but their leaching behavior leads to the fast deactivation of the catalyst and constitutes a second source of pollution [13]; and (3) nonmetals (N, B, S, F, and C) able to extend optical absorption of TiO_2 to the visible light region and then to improve visible-light-driven photocatalytic processes [14, 15]. Among the above-mentioned nonmetals, the most suitable and commonly used is nitrogen.

Nitrogen, as sulfur and fluorine species, is an anionic dopant which confers greater stability to the catalyst with respect to the conventional transition-metal dopants and also determines a significant red shift of the band gap into the visible range. According to theoretical modelling [16], the p-orbitals of the nitrogen dopant extensively overlapped, favouring the transfer of photogenerated charge carriers to the TiO_2 surface, in turn increasing its photocatalytic activity [17]. It was proven that both in the anatase and rutile phases of TiO_2, the N2p states were located just above the top of the O2p valence band, which means a red shift of the absorption band edge to the visible region [18].

Despite the potential, data about the main changes provided by nitrogen doping in TiO_2 is not well established. Moreover, for large scale usage of $TiO_{2-x}N_x$ nanomaterials in all the solar radiation ranges, none of the results actually reached are satisfactory due to their low nitrogen/oxygen content, low chemical-physical stability, and increased carrier trapping.

There are multiple and assorted methods to prepare N-TiO_2 catalysts. Physical vapor deposition (PVD), reactive sputtering, cathodic arc deposition, plasma-gas reaction, and Chemical Vapor Deposition (CVD) are the common methods used to deposit N-doped titania films. However, all these techniques allow the deposition of low level N-doped titania with micron-sized structures only at high vacuum conditions (10^{-8}-10^{-9} Pa) and at high temperature (1200-1500°C) to avoid sample reoxidation. The methods based on plasma-gas phase reactions with the use of TiN powders seem to be a good and low cost alternative to obtain films with a small particle size (about 10 nm). However, these samples show a high oxygen content (ca. 15–20 at.%) [19]. Recently TiO_2, loading a different percentage of nitrogen, was prepared by nitridation of a nano-TiO_2 powder in a mixed ammonia/argon atmosphere at a range of temperatures from 400 to 1100°C [17]. According to the results obtained by Zhang et al. [20], the samples prepared at 700°C are oxygen deficient, which may be partly responsible for the shifting band gap and for the significant photocatalytic activity. On the other hand, nanocolloid production generally involves the use of surfactants and derivatives which cause secondary pollution to the environment.

For all these reasons, further studies will be useful mainly to (1) clarify whether oxygen deficiency has a bigger effect on photocatalytic activity than N-doping at low levels, (2) give a systematic and complete characterization of the chemical-morphological and optical properties of the synthesized N-TiO_{2-x} nanomaterials, and (3) identify green methods and define a synthesis protocol in order to produce nanocolloids. This latter should be usable directly in the liquid phase in an innovative photocatalytic device, with a high degradation time (even in extreme conditions).

In this work, we presented and discussed the results obtained using the potentiality of the pulsed laser ablation in liquid (PLAL) technique to prepare N-TiO_{2-x} nanocolloids. The syntheses were carried out in water to favour the formation of (Ti-O-N), ($-NH_2$), NO_2^-, N_2, NH_x, and ($-OH$) species, inducing their incorporation into the TiO_2 lattice as nitride through dehydration. To this aim, the optimal PLAL deposition parameters (i.e., laser fluence and irradiation time) were found as well as the optimal composition of the targets (TiO_2 mixed to TiN powders or TiN rod purchased from Matek Srl). PLAL processes were performed in ambient condition (room temperature) using the water as solvent, with the advantage to obtain nanocolloids, without by-products, suitable for mechanical deposition on photoanode materials or to be incorporated in integrated solar water-splitting devices.

All the synthesized colloids were characterized by scanning transmission electron microscopy (STEM), X-ray photoelectron (XPS), and conventional optical spectroscopies, providing complementary information which allows drawing a picture of the compositional, morphological, and optical properties of the nanocomposites, constituting the starting point for their successive photocatalysis applications which require moderate operating temperatures and limited energy consumptions.

2. Experimental Section

$TiO_{2-x}N_x$ powders, pressed into a disk at room temperature, were prepared starting from powders of TiN and TiO_2 (P25), mixed at the TiN/TiO_2 mass ratios of 75/25, 50/50, and

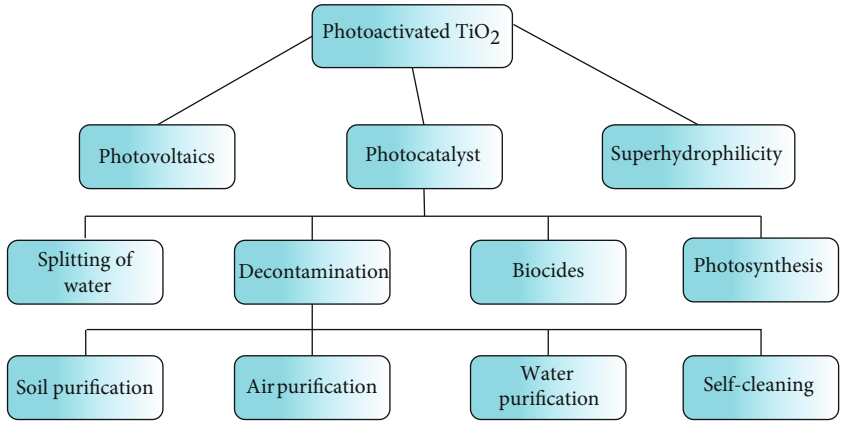

Figure 1: Dependence graph of photo-activated TiO_2 materials applications. The flow goes from the top to the bottom direction.

25/75. Then, the compacts were maintained in a furnace at around 250°C for 1 hour. Pulsed laser ablation in liquid (PLAL) processes of the pressed powders as well as of commercial TiN and TiO_2 rod targets (synthesized by Matek Srl at 1200°C) were carried out in deionized water (H_2O). The targets were irradiated at the laser fluence of 0.5 J/cm^2 for an irradiation time of 15 min (samples labelled TION3-5 and TION1P-5P-17P-12P) and of 1.5 J/cm^2 for 30 min (TION4), by the 532 nm radiation coming from a Nd:YAG laser source, operating at the repetition rate of 10 Hz and at the pulse width of 6 ns. The scheme of the PLAL setup and an overview of the sample set are shown in Figure 2.

Scanning transmission electron microscopy (STEM) images were acquired using a Zeiss electronic microscope which operates at an accelerating voltage of 30 kV. Samples for the STEM analysis were prepared by dropping a suspension of the sonicated colloids on a 400 mesh holey-carbon support sputter-coated with chromium.

A PerkinElmer (Lambda 750) spectrometer, working in the 300-900 nm range, was used to collect optical absorbance spectra.

The crystalline phase of the oxide was also investigated by analyzing Raman scattering data. Raman spectra have been excited with the 532 and 638 nm diode laser lines mounted in the XploRA spectrometer coupled with an Olympus microscope. Spectra have been collected with a 50x objective (spot size of about 2 μm) and a Charged Coupled Device (CCD) used as a sensor. An acquisition time of 80 s granted a sufficient S/N ratio.

The chemical bonding states and the relative atomic content in the nanocomposites were investigated by X-ray Photoelectron Spectroscopy (XPS), using the Thermo Scientific K-Alpha system equipped with a monochromatic Al-Kα source (1486.6 eV) and operating with a pass energy of 50 eV in the CAE mode.

Some aqueous solutions of methyl orange (MO) and methylene blue (MB) (Sigma-Aldrich) were prepared by dissolving the analytical grade dyes in the synthesized colloids at a $1.5 \cdot 10^{-5}$ M concentration.

MO and MB were used as probe molecules for a first evaluation of the photocatalytic activities of N-TiO_2 nanostructures. The reaction was conducted in 3 ml of aqueous solution containing the dye, previously maintained in a beaker for 30 min at a temperature of about 10°C. The photocatalytic reaction was carried out under stirring. 0.5 mg of catalyst was dispersed in 3 ml of dye aqueous solution placed in an ice bath; in this way, the temperature of aqueous dispersion was maintained at around 14 ± 2°C.

A 40 W Hg lamp (for UV irradiation) and a 450 W xenon lamp (as a visible light source blocking UV radiation by a 400 nm glass filter) were used as light sources placed at a distance of about 15 cm. Prior to irradiation, the dye catalyst suspensions were kept in the dark for 30 min to ensure an adsorption/desorption equilibrium. Then, the photodecolourization of MO and MB was studied.

Analytical samples were filtered through a 0.2 μm Millipore® filter to remove the solid, at well-defined time intervals during the irradiation, and placed into a 0.35 ml microquartz cuvette. Then, the residual dye concentrations in the filtrates were analyzed by UV-visible spectrophotometer (PerkinElmer 750) at maximum absorption wavelengths (λ_{max}) of 464 and 664 nm for MO and MB, respectively. Direct photolysis decolourization of the respective dye was estimated by performing blank experiments.

3. Results and Discussion

3.1. Sample Characterization. In Figure 3 are shown representative STEM images of the samples obtained ablating in water targets of different nature. Specifically, the colloids, obtained ablating the (25/75) TiN/TiO_2 powder targets, show a porous morphology with some spherical nanostructures with a mean diameter of about 50 nm (Figure 3(a)). It is to be noted that the observation of perfectly rounded submicrometer particles, probably associated with TiO_2 species, is in agreement with what was observed by Felice et al. [21]. On the other hand, a high density of nanoparticles with a spherical shape and size mainly below 30 nm characterizes the colloids prepared ablating the high purity (99.99%) commercial TiN rod target (Figure 3(c)). An analogous morphology is shown by the colloids prepared ablating the TiN powder target (Figure 3(b)). More details can be observed

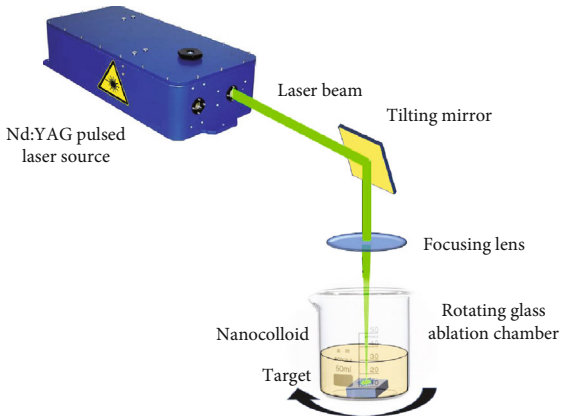

Sample	Preparation conditions
TION1P	From TiN powder (F = 0.5 J/cm^2; t = 15 min)
TION5P	From TiN/TiO_2 powder at 25/75 mass ratio (F = 0.5 J/cm^2; t = 15 min)
TION12P	From TiN/TiO_2 powder at 75/25 mass ratio (F = 0.5 J/cm^2; t = 15 min)
TION17P	From TiN/TiO_2 powder at 50/50 mass ratio (F = 0.5 J/cm^2; t = 15 min)
*Ti*ON3	From TiN target (F = 0.5 J/cm^2; t = 15 min)
*Ti*ON4	From TiN target (F = 1.5 J/cm^2; t = 15 min)
*Ti*ON5	From TiN target (F = 0.5 J/cm^2; t = 30 min)

Figure 2: Scheme of PLAL setup and synthesis parameters for each adopted target.

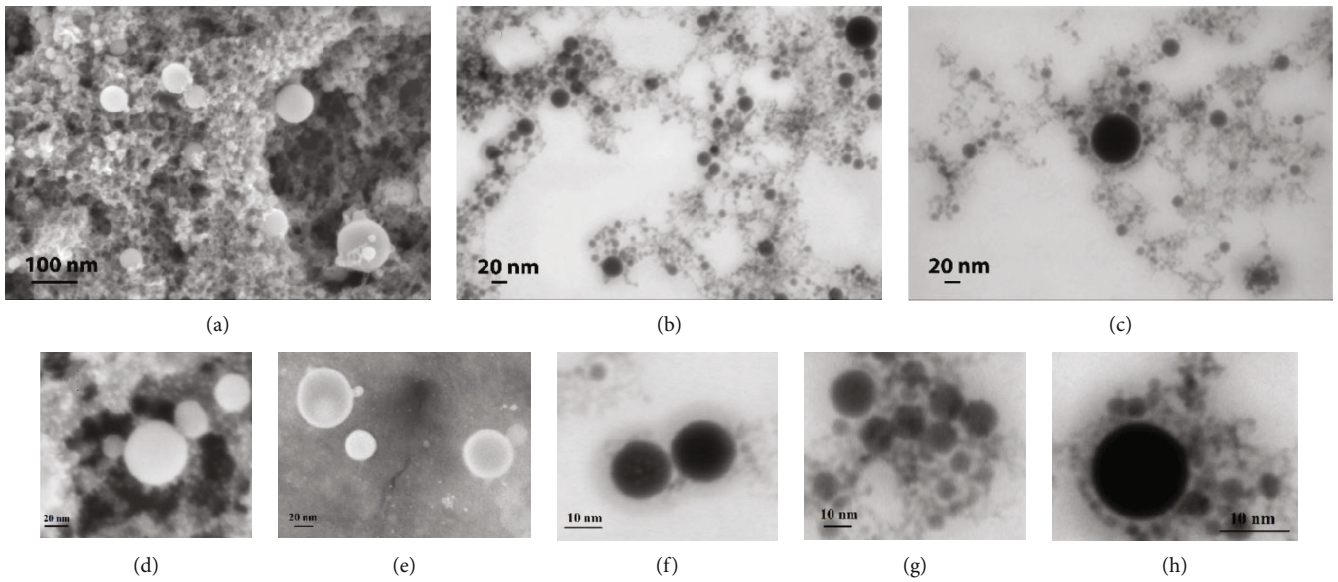

Figure 3: STEM images of the samples obtained ablating the (25/75) TiN/TiO_2 powder targets (a, d, e), the TiN powder target (b, f), and the high purity (99.99%) commercial TiN rod target (c, g, h).

from images d–h collected for the samples obtained ablating the (25/75) TiN/TiO_2 powder targets and the TiN rod and powder targets.

The sample obtained from the (25/75) mixed TiN/TiO_2 powders show Raman features typical of the anatase-rich TiO_2 material [6]. It is important to highlight that first-order Raman features of TiN (at 225 cm^{-1} (TA), 310 cm^{-1} (LA), and 540 cm^{-1}(TO)) are almost absent, suggesting that nitrogen could be incorporated as a defect in the crystalline TiO_2 lattice. Samples, obtained from TiN powder (red line) and rod (blue line) targets, showed very similar Raman spectra; in this case, TiN vibrational features are well observable (see Figure 4(a)) as indicated by the pronounced peak at about 550 cm^{-1} related to the TiN-TO mode [22]. Moreover, we observe that the E_g (associated to the anatase phase) signal below 200 cm^{-1} is totally absent and that the intensity ratio between the observed peaks at 200 and 290 cm^{-1} is very similar to that of a possible formation of a rutile TiO_2 phase. Unfortunately, TiN and rutile features overlapped in this region, so a correct attribution for the rutile is not possible exclusively from Raman analyses. All this evidence indicates a tendency towards an anatase-rutile conversion and/or an oxygen replacement by nitrogen with the formation of Ti-N bonds [22]. Interstitial nitrogen species are expected as a result of the ablation of a TiN target in water.

In Figure 4(b) are shown the optical absorbance spectra of the synthesized nanocolloids. We observe that (1) the colloid obtained by a TiN rod target is transparent (over 90%) in the visible range with a sharp absorption edge at about 350 nm, (2) a broad band at around 420 nm characterizes the sample prepared from the TiO_2 powder target, and (3) a slight blue shift is evident in the colloids prepared using the pressed and sintered target with a (75/25) TiN/TiO_2 mass ratio; for these samples, the 420 nm band is totally absent, while a significant visible light absorption contribution up to 600 nm is evident, probably due to the electronic transition from the localized N doping level to the conduction band of TiO_2 (see also the scheme reported in Figure 5).

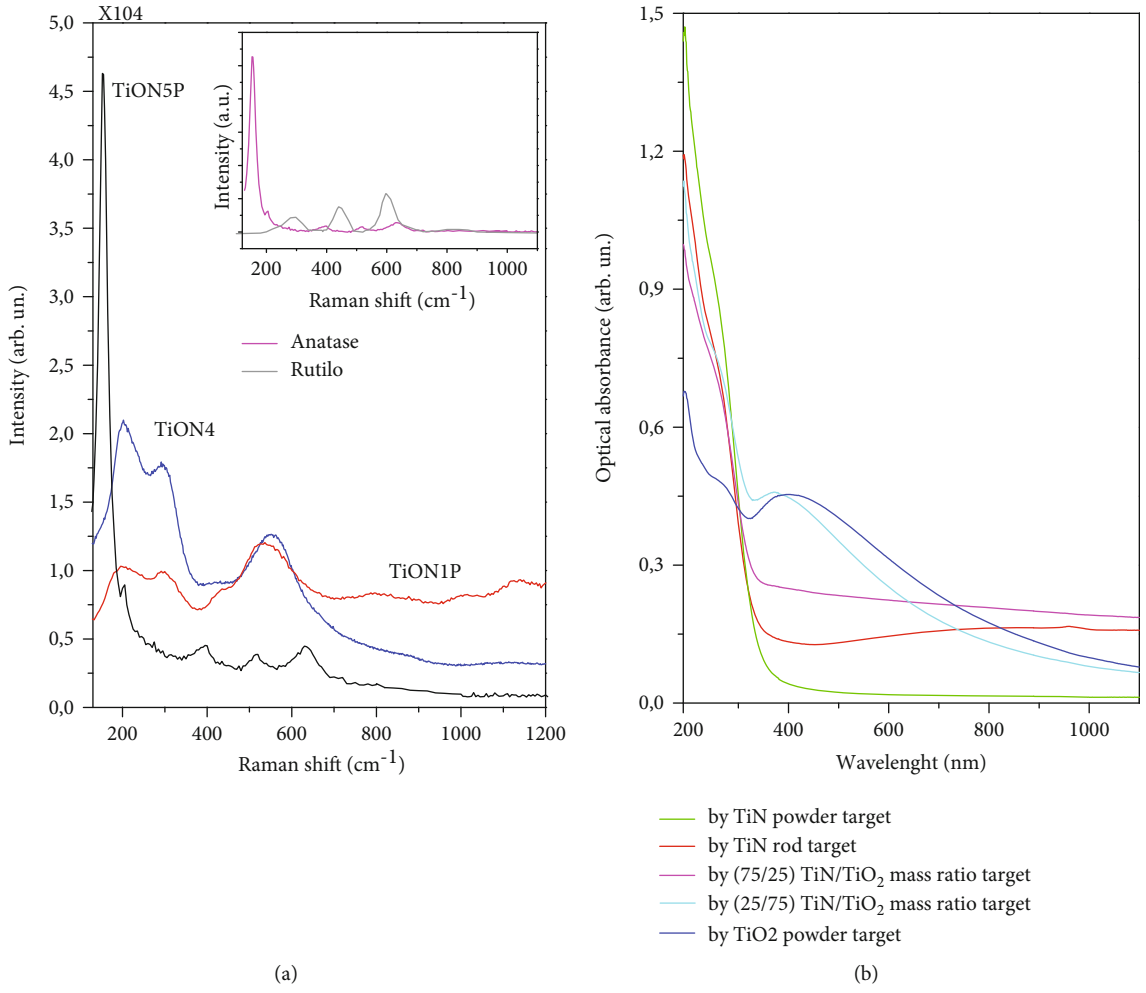

Figure 4: (a) Raman and (b) optical absorbance spectra of the synthesized samples.

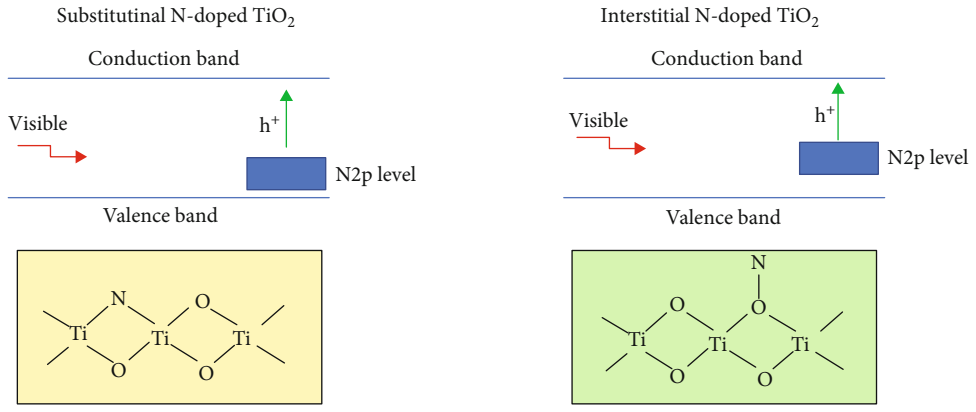

Figure 5: Schematic diagram showing the valence and conduction bands of N-doped TiO_2.

The incorporation of nitrogen into the TiO_2 lattice leads to the formation of a new midgap energy state, i.e., the N2p band above the O2p valence band. So, upon a visible light irradiation, the electrons can migrate from the valence band to the conduction band (Figure 5) and from here the expected visible light activity of N-dopedTiO_2 or $TiO_{2-x}N_x$ materials (see Catalytic Activities). Nitrogen can replace one or more oxygen atoms ("substitutional doping"), or nitrogen can be positioned in interstitial TiO_2 sites ("interstitial doping"). In both cases, as shown in Figure 5, N doping

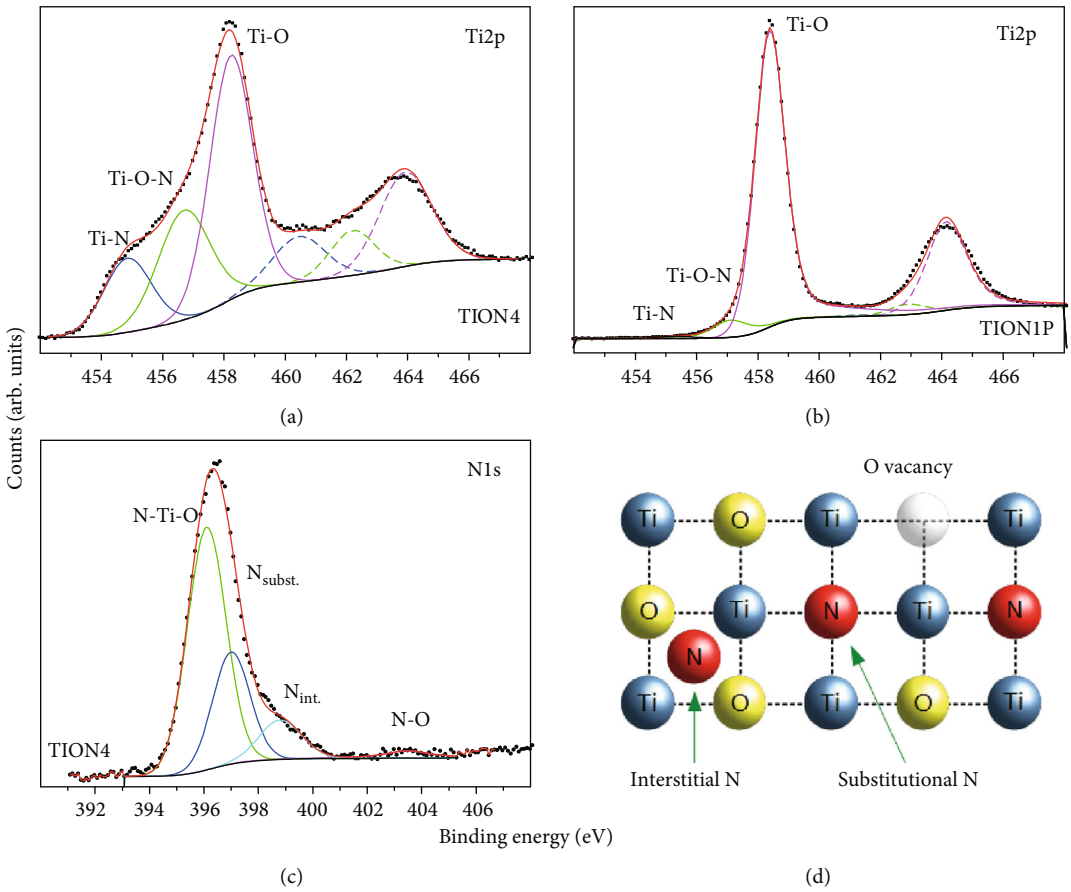

FIGURE 6: Ti2p (a, b) deconvoluted profiles of the samples obtained from the TiN rod and TiN powder targets, respectively. We outline that all the samples obtained from the mixed powders show Ti2p line shapes similar to those of the sample starting from the TiN powder. The N1s deconvoluted profile of the sample obtained starting from the TiN rod target (c) and a scheme of the potential nitrogen allocation into the TiO_2 structure (d).

TABLE 1: Atomic surface chemical composition and bonding fraction estimated by the deconvoluted XPS spectra.

Sample	Chemical composition (%)			Bonding configurations (%)						
				Ti2p			N1s			
	N (%)	Ti (%)	O (%)	Ti-N	Ti-O-N	$Ti-O_2$	N-Ti-O	$N_{subst.}$	$N_{int.}$	NO/NO_2
TION1p	1.1	28.8	70.1	0.8	6.4	92.8	—	—	100	—
TION5p	0.7	28.4	71.0	0.5	3.5	96.0	—	—	100	—
TION12p	5.9	23.8	70.3	0.9	3.4	95.7	—	—	100	—
TION17p	4.6	19.8	75.6	0.0	3.7	96.3	—	—	100	—
TION3	12.2	28.8	59.1	15.5	26.0	58.5	67.4	18.5	9.5	4.6
TION4	17.8	24.1	58.1	17.8	29.1	53.1	59.7	26.6	10.7	2.9
TION5	14.8	25.7	59.6	17.4	30.1	52.6	65.5	22.0	9.9	2.7

leads to a change in the electronic behavior of the nanoparticle due to a change in the electronic band structures and/or a decrease of electron-hole recombination [23].

XPS analysis allows investigating the surface chemical composition and bonding configurations of our samples, in which it is known that the surface chemical coordination greatly influences the catalytic response [24]. In Figures 6(a)–6(c) are shown representative Ti2p and N1s deconvoluted profiles, while the chemical atomic percentage of the detected species and the relative surface bonding configurations are reported in Table 1. Two different Ti2p profiles characterize our samples: those obtained starting from the TiN rod target (Figure 6(a)) show a broad band whose features are ascribed to the titanium nitride, the titanium dioxide (TiO_2), and the intermediate phase of titanium oxynitride [25, 26]. Otherwise, in the samples obtained by the TiN powder (Figure 6(b)), narrower profiles are obtained and the binding energy of the $Ti2p_{3/2}$ peak is brought closer

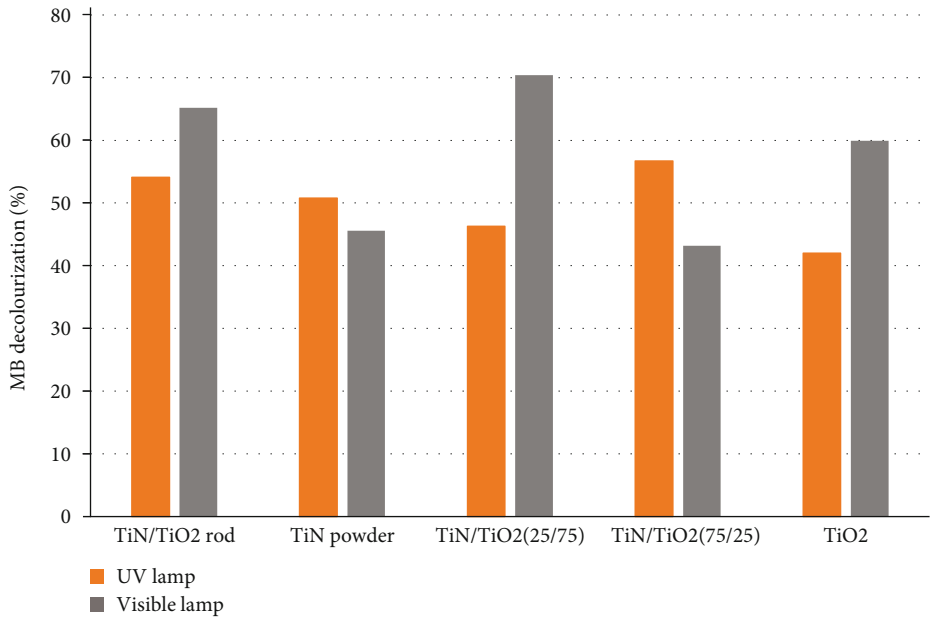

Figure 7: Photocatalytic activity towards the methylene blue (MB) dye molecule under UV and visible irradiation (60 min exposure time).

to 458.5 eV (typical of TiO_2 compound), while the binding energies of the other phases still fall within the possible ranges. Interestingly, no resolved N1s signal was collected from the powder targets while the N1s profile is well structured and defined for samples obtained from the rod targets (Figure 6(c)). The main components are located at around 396 and in the 397-400 eV range. These features are ascribed to the titanium oxynitride phase and to the nitrogen in substitutional and interstitial positions [26–31]. The NH_x, NO/NO_2, and NO^{3-} contributions are generally reported at a binding energy higher than 400 eV [29–31] but, in our case, are less pronounced (see Figures 6(c) and 6(d)).

3.2. Catalytic Activities. All the photocatalytic reactions were undertaken in air as the photobleaching of MB is irreversible in an oxygen-saturated aqueous solution such as ours, and in an ice bath to avoid degradation effects due to light irradiation-induced heating. The photodegradation was monitored by recording UV-visible extinction spectra as a function of light irradiation exposure time. The percentage of MB decolourization under ultraviolet and visible radiation for the synthesized and TiO_2 reference samples is shown in Figure 7. Under UV and visible irradiation, all the produced nanostructures show a photocatalytic activity towards the degradation of methylene blue (MB) dye molecule. However, the response is comparable in all the samples under UV irradiation while, under the visible lamp, the estimated percentages differ by about 30%. In fact, for the samples obtained by ablating TiN powder and TiN/TiO_2-mixed powder in 75/25 ratio, MB decolourization is about 45% but increases in the samples obtained from the TiN rod or from the TiN/TiO_2-mixed powders at the 25/75 ratio. Photocatalytic decolourization behavior of MB dye (during visible irradiation, over the 1 h time frame of the experiment) seems to be influenced by the amount of N, Ti, and O and their bonding coordination and by the increasing absorption in the visible light region [32].

In Figure 8 is shown the percentage of MO decolourization under UV and visible lamp for the synthesized and reference samples. MO is an azo dye characterized by a N=N linkage, which is anionic in aqueous media and absorbs light in the visible region (450–550 nm) with an absorption maxima at 464 nm [33]. The samples obtained by TiN rod or TiN powder targets as well as those in which the TiN fraction is higher than the TiO_2 one (75/25 ratio) are the most active nanocomposites, both under UV and visible irradiation. For the colloids going from the TiN rod, we observe that, in the first 20 min, 50% and 60% of the dye were removed under UV and visible light, respectively, while only about 10% of the dye is removed for the TiO_2 colloid. Moreover, 70% of MO decolourization occurs within 80 min under visible irradiation while the other samples, for which Ti-O chemical bonds dominate in comparison to TiN/Ti-O-N ones, show significantly less efficiency in the same range of time.

In order to have a quantitative estimation of the photocatalytic activity, we carried out a simple fitting procedure already adopted to test photodegradation efficiency of MB using zinc oxide nanocolloids, prepared by picosecond pulsed laser ablation, as catalysts [34]. If a semilogarithm scale of the relative absorbance as function of irradiation time is employed, it is possible to obtain a pseudoorder constant rate for all analyzed samples (see Table 2). In detail, by following the equation

$$\ln\left(\frac{A}{A_0}\right) = -k_c t, \tag{1}$$

with A_0 and A_t as the starting absorbance and the absorbance at the time t, respectively, a linear fitting procedure, limited

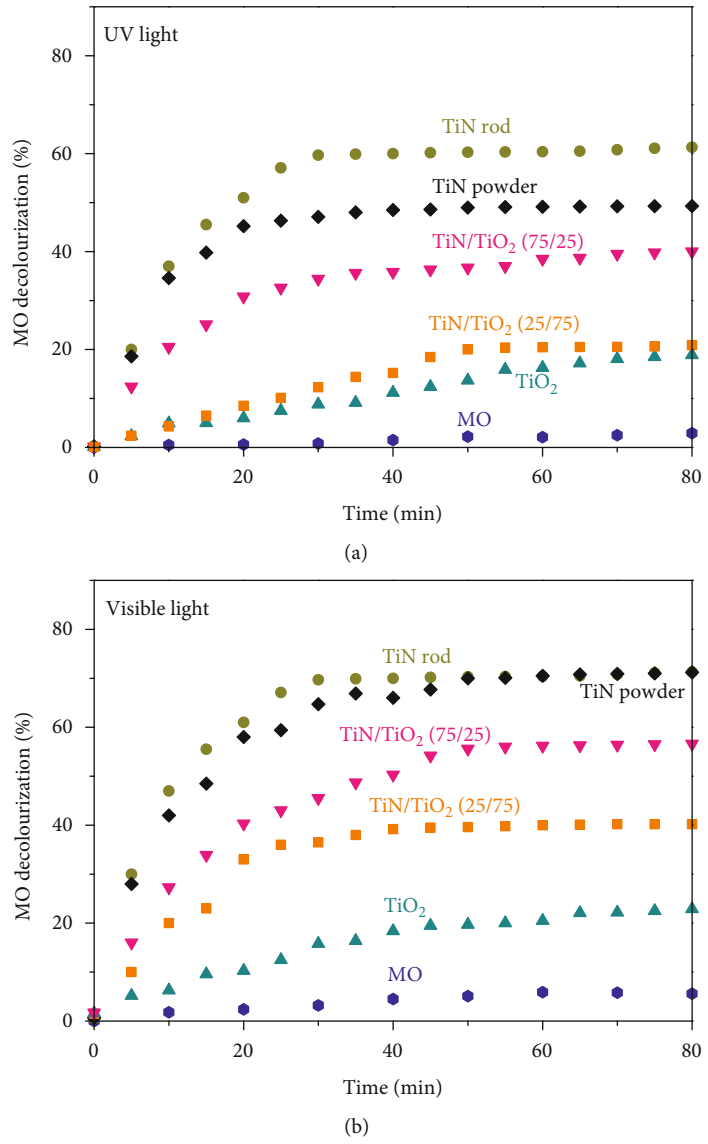

Figure 8: Photocatalytic activity towards the methyl orange (MO) dye molecule under UV and visible irradiation (60 min exposure time).

Table 2: Photodegradation rate constants of MB and MO with different catalysts using $\ln(A/A_0) = -k_c t$ as the fitting equation model.

Sample	k_c (min^{-1})			
	MB		MO	
	UV lamp	Visible lamp	UV lamp	Visible lamp
TION5 (TiN rod target)	-0.0118	-0.0211	-0.0333	-0.0426
TION1P (TiN powder target)	-0.0129	-0.0126	-0.0300	-0.0326
TION5P (TiN/TiO_2 (25/75) target)	-0.0103	-0.0242	-0.0043	-0.0176
TION12P (TiN/TiO_2 (75/25) target)	-0.0139	-0.0113	-0.0153	-0.0158
TiO_2 target	-0.0091	-0.0211	-0.0026	-0.0046

to the first 30 minutes of irradiation, is evidence that both dyes degrade faster under the visible source and that the highest k_c value is obtained with nanocatalysts from the TiN rod target.

Hence, on the basis of the obtained results, we suggest that the sample obtained from TiN characterized by the higher N content could be photosensitized by the "N-doping." In this case, oxygen vacancies promoted the charge recombination, resulting in weak reduction power. Otherwise, the high activity of the sample synthesized from the TiN/TiO_2 mixed powder in 25/75 ratio was attributed to the abundance of hydroxy groups in its porous structure

(see STEM image), which provided more active sites for the degradation reaction as well as to the high available surface/-volume ratio of the catalyst, since this sample shows a porous structure (Figure 3(a)). Nevertheless, no clear correlation between the MB or MO photocatalytic activity and the chemical-structural properties of the synthesized nanocolloids is found, since dye decolourization is also affected by the ionic nature, structure and stability, adsorption, and orientation of the dye molecules on the surface of the catalyst [35, 36]. The synthesized N-TiO_2 nanocatalysts should be further investigated in depth to improve their catalytic response in the visible spectral region by a more rational and environment-friendly PLAL approach.

4. Conclusions

In this work, the potentiality of the pulsed laser ablation in liquid (PLAL) technique to prepare N-TiO_{2-x} nanocolloids, suitable for mechanical deposition on photoanode materials by conventional spraying technique, or to be incorporated in integrated solar water-splitting devices was reported. Synthesis processes were carried out in water, using targets with different nature and composition, to favour the formation of (Ti-O-N), ($-NH_2$), NO^{2-}, N_2, NH_x, and (−OH) species, and the nitrogen incorporation into the TiO_2 lattice as nitride through dehydration. PLAL processes were performed in ambient condition (room temperature) using the water as solvent, without the need to provide high temperature (T) and pressures (P), thus preparing nanocolloids, ready to use without by-products. The observed photoactivity response of the synthesized nanocatalysts is explained in terms of their surface composition and bonding configurations and optical and morphological properties, which has been tuned changing the incorporation of nitrogen into the TiO_2 lattice, beneficial for potentially separating the photogenerated carriers in space.

Data Availability

The data used to support the reported findings are available from the corresponding authors upon request.

Conflicts of Interest

The authors declare that they have no conflicts of interest.

References

[1] Y. Lan, Y. Lu, and Z. Ren, "Mini review on photocatalysis of titanium dioxide nanoparticles and their solar applications," *Nano Energy*, vol. 2, no. 5, pp. 1031–1045, 2013.

[2] C. F. Goodeve and J. A. Kitchener, "The mechanism of photosensitisation by solids," *Transactions of the Faraday Society*, vol. 34, pp. 902–908, 1938.

[3] K. Hashimoto, H. Irie, and A. Fujishima, "TiO_2 photocatalysis: a historical overview and future prospects," *Japanese Journal of Applied Physics*, vol. 44, no. 12, pp. 8269–8285, 2005.

[4] M. Liu, "Water photolysis with a cross-linked titanium dioxidenanowire anode," *Chemical Science*, vol. 2, no. 1, pp. 80–87, 2011.

[5] S. Al Jitan, G. Palmisano, and C. Garlisi, "Synthesis and surface modification of TiO_2-based photocatalysts for the conversion of CO_2," *Catalysts*, vol. 10, no. 2, p. 227, 2020.

[6] M. Ni, M. K. H. Leung, Y. C. D. Leung, and K. Sumathy, "A review and recent developments in photocatalytic water-splitting using TiO_2 for hydrogen production," *Renewable and Sustainable Energy Reviews*, vol. 11, no. 3, pp. 401–425, 2007.

[7] M. E. Borges, M. Sierra, E. Cuevas, R. D. García, and P. Esparza, "Photocatalysis with solar energy: sunlight-responsive photocatalyst based on TiO_2 loaded on a natural material for wastewater treatment," *Solar Energy*, vol. 135, pp. 527–535, 2016.

[8] S. Banerjee, D. D. Dionysiou, and S. C. Pillai, "Self-cleaning applications of TiO_2 by photo-induced hydrophilicity and photocatalysis," *Applied Catalysis B: Environmental*, vol. 176, pp. 396–428, 2015.

[9] A. Fujishima, T. N. Rao, and D. A. Tryk, "Titanium dioxide photocatalysis," *Journal of Photochemistry and Photobiology C*, vol. 1, no. 1, pp. 1–21, 2000.

[10] N. Sofyan, A. Ridhova, A. H. Yuwono, and A. Udhiarto, "Fabrication of solar cells with TiO_2 nanoparticles sensitized using natural dye extracted from mangosteen pericarps," *International Journal of Technology*, vol. 6, pp. 1229–1238, 2017.

[11] S. Filice, D. D'Angelo, S. F. Spanò et al., "Modification of graphene oxide and graphene oxide–TiO2 solutions by pulsed laser irradiation for dye removal from water," *Materials Science in Semiconductor Processing*, vol. 42, pp. 50–53, 2016.

[12] P. Wang, B. Huang, Y. Dai, and M. Whangbo, "Plasmonic photocatalysts: harvesting visible light with noble metal nanoparticles," *Physical Chemistry Chemical Physics*, vol. 14, no. 28, pp. 9813–9825, 2012.

[13] M. Pelaez, "A review on the visible light active titanium dioxide photocatalysts for environmental applications," *Applied Catalysis B: Environmental*, vol. 125, pp. 331–349, 2012.

[14] J. G. Yu, G. P. Dai, Q. J. Xiang, and M. Jaroniec, "Fabrication and enhanced visible-light photocatalytic activity of carbon self-doped TiO2sheets with exposed {001} facets," *Journal of Materials Chemistry*, vol. 21, no. 4, pp. 1049–1057, 2011.

[15] X. H. Tangand and D. Y. Li, "Sulfur-doped highly ordered TiO_2 nanotubular arrays with visible light response," *Journal of Physical Chemistry C*, vol. 112, no. 14, pp. 5405–5409, 2008.

[16] R. Asahi, T. Morikawa, T. Ohwaki, K. Aoki, and Y. Taga, "Visible-light photocatalysis in nitrogen-doped titanium oxides," *Science*, vol. 293, no. 5528, pp. 269–271, 2001.

[17] W. Y. Choi, A. Termin, and M. R. Hoffmann, "The role of metal ion dopants in quantum-sized TiO2: correlation between photoreactivity and charge carrier recombination dynamics," *The Journal of Physical Chemistry*, vol. 98, no. 51, pp. 13669–13679, 2002.

[18] C. D. Valentin, G. Pacchioni, and A. Selloni, "Origin of the different photoactivity of N-doped anatase and rutile TiO_2," *Physical Review B*, vol. 70, article 085116, 2004.

[19] J. R. Groza, J. D. Curtis, and M. Kramer, "Field-assisted sintering of nanocrystalline titanium nitride," *Journal of the American Ceramic Society*, vol. 83, no. 5, pp. 1281–1283, 2000.

[20] Z. Zhang, J. B. M. Goodall, D. J. Morgan et al., "Photocatalytic activities of N-doped nano-titanias and titanium nitride,"

Journal of the European Ceramic Society, vol. 29, no. 11, pp. 2343–2353, 2009.

[21] S. Filice, G. Compagnini, R. Fiorenza et al., "Laser processing of TiO_2 colloids for an enhanced photocatalytic water splitting activity," *Journal of Colloid and Interface Science*, vol. 489, pp. 131–137, 2017.

[22] M. Franck, J.-P. Celis, and J. R. Roos, "Microprobe Raman spectroscopy of TiN coatings oxidized by solar beam heat treatment," *Journal of Materials Research*, vol. 10, no. 1, pp. 119–125, 1995.

[23] S. A. Ansari, M. M. Khan, M. O. Ansaric, and M. H. Cho, "Nitrogen-doped titanium dioxide (N-doped TiO_2) for visible light photocatalysis," *New Journal of Chemistry*, vol. 40, no. 4, pp. 3000–3009, 2016.

[24] D. S. García-Zaleta, A. M. Torres-Huerta, M. A. Domínguez-Crespo, A. García-Murillo, R. Silva-Rodrigo, and R. L. González, "Influence of phases content on Pt/TiO_2, Pd/TiO_2 catalysts for degradation of 4-chlorophenol at room temperature," *Journal of Nanomaterials*, vol. 2016, Article ID 1805169, 15 pages, 2016.

[25] https://xpssimplified.com/elements/titanium.php.

[26] D. Kusano, M. Emori, and H. Sakama, "Influence of electronic structure on visible light photocatalytic activity of nitrogen-doped TiO_2," *RSC Advances*, vol. 7, no. 4, pp. 1887–1898, 2017.

[27] V. Diesen, C. W. Dunnill, J. C. Bear, S. Firth, M. Jonsson, and I. P. Parkin, "Visible light photocatalytic activity in AACVD-prepared N-modified TiO_2 thin films," *Chemical Vapor Deposition*, vol. 20, no. 1-3, pp. 91–97, 2014.

[28] X. Cheng, X. Yu, Z. Xing, and J. Wan, "Enhanced photocatalytic activity of nitrogen doped TiO_2 anatase nano-particle under simulated sunlight irradiation," *Energy Procedia*, vol. 16, pp. 598–605, 2012.

[29] R. Quesada-Cabrera, C. Sotelo-Vázquez, M. Quesada-González, E. P. Melián, N. Chadwick, and I. P. Parkin, "On the apparent visible-light and enhanced UV-light photocatalytic activity of nitrogen-doped TiO_2 thin films," *Journal of Photochemistry and Photobiology A: Chemistry*, vol. 333, pp. 49–55, 2017.

[30] B. Tryba, M. Wozniak, G. Zolnierkiewicz et al., "Influence of an electronic structure of $N\text{-}TiO_2$ on its photocatalytic activity towards decomposition of acetaldehyde under UV and fluorescent lamps irradiation," *Catalysts*, vol. 8, no. 2, p. 85, 2018.

[31] N. T. Nolan, D. W. Synnott, M. K. Seery, S. J. Hinder, A. Van Wassenhovend, and S. C. Pillai, "Effect of N-doping on the photocatalytic activity of sol–gel TiO_2," *Journal of Hazardous Materials*, vol. 211-212, pp. 88–94, 2012.

[32] W. Kallel, S. Chaabene, and S. Bouattour, "Novel (Ag,Y) doped TiO_2 plasmonic photocatalyst with enhanced photocatalytic activity under visible light," *Physicochemical Problems of Mineral Processing*, vol. 55, no. 3, pp. 745–759, 2019.

[33] T. T. Minh, N. T. T. Tu, T. T. Van Thi et al., "Synthesis of porous octahedral ZnO/CuO composites from Zn/Cu-based MOF-199 and their applications in visible-light-driven photocatalytic degradation of dyes," *Journal of Nanomaterials*, vol. 2019, Article ID 5198045, 16 pages, 2019.

[34] L. D'Urso, S. Spadaro, M. Bonsignore et al., "Zinc oxide nanocolloids prepared by picosecond pulsed laser ablation in water at different temperatures," *EPJ Web of Conferences*, vol. 167, article 04008, 2018.

[35] B. Wei, F. Tielens, and M. Calatayud, "Understanding the role of rutile TiO_2 surface orientation on molecular hydrogen activation," *Nanomaterials*, vol. 9, no. 9, article 1199, 2019.

[36] V. Vaissier, V. G. Sakai, X. Li, J. T. Cabral, J. Nelson, and P. R. F. Barnes, "How mobile are dye adsorbates and acetonitrile molecules on the surface of TiO_2 nanoparticles? A quasi-elastic neutron scattering study," *Scientific Reports*, vol. 6, no. 1, article 39253, 2016.